URSI AP-RASC 2019, New Delhi, India; 09 - 15 March 2019

Enhanced ADO-OFDM with Subcarrier Resource Allocation for Heterogeneous Networks

Xuan Huang[(1)], Fang Yang*[(1)(2)], and Jian Song[(1)(2)]
(1) Department of Electronic Engineering, Tsinghua University,
Beijing National Research Center for Information Science and Technology (BNRist), Beijing 100084, P. R. China
(2) Key Laboratory of Digital TV System of Guangdong Province and Shenzhen City,
Research Institute of Tsinghua University in Shenzhen, Shenzhen 518057, P. R. China
Email: hx17@mails.tsinghua.edu.cn, fangyang@tsinghua.edu.cn, jsong@tsinghua.edu.cn

Abstract

In this paper, an enhanced asymmetrically clipped DC biased optical OFDM (ADO-OFDM) with adaptive subcarrier resource allocation is proposed to accommodate the requirements of multi-users in downlink multiple access. Additionally, the maximum achievable capacity of the enhanced ADO-OFDM system is investigated. Then, the optimization of optical power allocation for the enhanced ADO-OFDM with a limit on the total optical power is analyzed and formulated to maximize the total channel capacity. Simulation results show that the total channel capacity of the proposed scheme has a large increase compared with that of the schemes without power allocation.

1 Introduction

Recently, visible light communication (VLC), whose spectrum resource is unlicensed, has been emerging as a candidate to complement the conventional radio frequency (RF) counterpart. Additionally, VLC is regarded as a green communication because of its low power consumption. VLC has many distinctive advantages, such as huge bandwidth, low cost, and localization capability, which ensures its effectiveness for navigating, timing, and positioning systems [1]. Besides, in the physical layer, VLC and RF communications are compatible and can be regarded as heterogeneous networks.

For the optical orthogonal frequency division multiplexing (OFDM)-based wireless communication system with intensity modulation and direct detection (IM/DD), the instantaneous time-domain signal is modulated on the intensity of the LEDs, so the transmitted signal requires to be real, which can be ensured by the Hermitian symmetry, and nonnegative [2]. The capacity for the OFDM-baised optical wireless communication systems has been investigated by many researchers. For example, in literature [3], a new mathematical approximation method for the intrinsic volumes of the simplex is proposed to derive a tight sphere-packing upper bound on channel capacity. Further, the calculations for ACO-OFDM are extended to the case of a frequency selective channel [4].

In this paper, an enhanced ADO-OFDM scheme with subcarrier resource allocation is proposed first, in which the numbers of subcarriers occupied by ACO-OFDM and DCO-OFDM can be adaptively adjusted according to the different access demands of services in downlink multiple access. In addition, the optimization of optical power allocation under the constraint of normalized total optical power. Simulation results show that the channel capacity of the proposed scheme increases significantly compared with the schemes without power allocation.

The rest of this paper is organized as follows. In Section II, the conventional ADO-OFDM scheme is reviewed. In Section III, the enhanced ADO-OFDM scheme with subcarrier resource allocation and the optimal optical power allocation scheme are proposed. The simulation results are presented in Section IV. Finally, conclusions are drawn in Section V.

2 System Model

In ADO-OFDM, the ACO-OFDM signal is modulated on odd subcarriers while the DCO-OFDM signal is conveyed on even subcarriers [2]. The ACO-OFDM signal in the frequency domain can be formulated as

$$\mathbf{X}=\left[0,S_1,0,S_3,\cdots,S_{N/2-1},0,S^*_{N/2-1},\cdots,S^*_3,0,S^*_1\right], \quad (1)$$

where $(\cdot)^*$ denotes the operation of conjugation, N is the number of subcarriers. $S_n\left(0<n<N/2\right)$ is the symbol modulated on the n-th subcarrier and Hermitian symmetry is imposed. Then, the time-domain signal x_n can be obtained after the process of N-point inverse fast transform (IFFT). It has been proved that the negative part of x_n can be clipped without any information loss, while the clipping noise of ACO-OFDM only falls on the even subcarriers [5], which will not affect the demodulation process of data on the odd subcarriers.

On the other hand, for DCO-OFDM in ADO-OFDM

*Xuan Huang and Fang Yang contributed equally to this work.

scheme, after imposing Hermitian symmetry on the subcarriers, the frequency-domain signal can be denoted as

$$\mathbf{Y}=\left[0,0,S_2,0,\cdots,S_{N/2-2},0,0,0,S^*_{N/2-2},\cdots,0,S^*_2,0\right]. \quad (2)$$

Then, the time-domain signal y_n of DCO-OFDM can be obtained after the process of N-point IFFT. To make the time-domain signal of DCO-OFDM non-negative, a DC bias $B_{\mathrm{DC}}=\mu\delta_{DCO}$ is added to y_n, where μ and δ_{DCO} denote a proportional constant and the standard deviation of the DCO-OFDM signal in the time domain, respectively [2]. Like in [6], the bias is defined as $\beta=10\log_{10}\left(\mu^2+1\right)$ dB.

At the receiver, the ACO-OFDM signal is first demodulated as that implemented in ACO-OFDM. Then, the time-domain ACO-OFDM signal can be regenerated and subtracted to detect the remaining DCO-OFDM signal.

3 Proposed Schemes

3.1 Enhanced ADO-OFDM with Subcarrier Allocation

An enhanced ADO-OFDM scheme is proposed in this section, in which the numbers of subcarriers allocated to ACO-OFDM and DCO-OFDM are not fixed to $N/2$ and $N/2-2$ anymor. For the enhanced ADO-OFDM scheme, the number of odd subcarriers allocated to ACO-OFDM, represented as N_A, can be any even number from 2 to $N/2$, while the DCO-OFDM signal occupies the remaining N_D subcarriers, i.e.,

$$\begin{cases} N_A+N_D=N-2, \\ 2\le N_A\le N/2, \\ N/2-2\le N_D\le N-4. \end{cases} \quad (3)$$

Note N_A and N_D include both the data symbols and the corresponding Hermitian symmetries, respectively. In this paper, the N_A and N_D can be adjusted according to the users' requirements or the access conditions of services in downlink multiple access.

In enhanced ADO-OFDM, the ACO-OFDM signal is still only modulated on the odd subcarriers, which means the clipping noise of ACO-OFDM signal will only fall on the even subcarriers and will not interfere the detection for the data on the odd subcarriers. Hence, at the receiver, the ACO-OFDM and DCO-OFDM signal in the enhanced ADO-OFDM scheme can be detected as those in the conventional ADO-OFDM scheme, respectively.

3.2 Optimization of Optical Power Allocation

In this paper, the total optical power of ADO-OFDM is normalized to unity. Thus, the proportion of optical power allocated to ACO-OFDM is formulated as

$$\rho=\frac{P_{o,ACO}}{P_{o,ACO}+P_{o,DCO}}=P_{o,ACO}, \quad (4)$$

where $0\le\rho\le1$.

For the proposed enhanced ADO-OFDM, the channel capacity (or the maximum achievable capacity due to the real and positivity constraints of the VLC) can be formulated by

$$C=\frac{N_A}{2N}W\log_2\left(1+\frac{\sigma^2_{ACO}}{4\sigma^2_n}\right)+\frac{N-2-N_A}{2N}W\log_2\left(1+\frac{\sigma^2_{DCO}}{\sigma^2_n}\right), \quad (5)$$

where $\sigma^2_n=N_0W/N$ represents the variance of the AWGN with mean of zero, in which N_0 and W denote the noise power spectral density (PSD) and the occupied bandwidth, respectively. σ^2_{ACO} and σ^2_{DCO} are the effective electrical power for ACO-OFDM and DCO-OFDM in the proposed enhanced ADO-OFDM system, respectively. It can be derived that $\sigma^2_{ACO}=\beta_A\cdot\pi\rho^2$ and $\sigma^2_{DCO}=\beta_D\cdot(1-\rho)^2/D^2$, where $\beta_A=2N/N_A$, $\beta_D=N/N_D$, $D=\mu\left(1-Q\left(\mu\right)\right)+1/\sqrt{2\pi}\cdot\exp\left(-\mu^2/2\right)$, and $Q\left(x\right)=1/\sqrt{2\pi}\cdot\int_x^{\infty}\exp\left(-u^2/2\right)\mathrm{d}u$ [2] and [7].

The optimization objective is to find the optimal proportion of optical power allocated to ACO-OFDM to maximize the channel capacity, which is formulated as

$$\begin{aligned} &\rho_0=\arg\max_{\rho} C\left(\rho\right) \\ &\text{s.t. } 0\le\rho\le1 \end{aligned}. \quad (6)$$

The derivative of (5) is derived as

$$\frac{\partial C}{\partial\rho}=\frac{W}{N\ln2}\left(\frac{1}{f_1\left(\rho\right)}-\frac{1}{f_2\left(\rho\right)}\right), \quad (7)$$

where

$$f_1\left(\rho\right)=\rho+\frac{A}{\rho}, \quad (8)$$

and

$$f_2\left(\rho\right)=\frac{1}{K}\left(1-\rho+\frac{B}{1-\rho}\right), \quad (9)$$

in which $A=4\sigma^2_n/(\pi\beta_A)$, $B=D^2\sigma^2_n/\beta_D$, and $K=(N-2-N_A)/N_A$.

Obviously, $f_1\left(\rho\right)$ and $f_2\left(\rho\right)$ are double hook functions, and it can be derived that the asymptotes of $f_1\left(\rho\right)$ are $\rho=0$ and

$$g_1\left(\rho\right)=\rho, \quad (10)$$

while the asymptotes of $f_2\left(\rho\right)$ are $\rho=1$ and

$$g_2\left(\rho\right)=-\frac{\rho}{K}+\frac{1}{K}. \quad (11)$$

The graphs of the above functions are shown in Figure 1. Besides, the minimum value points of $f_1\left(\rho\right)$ and $f_2\left(\rho\right)$, denoted as point M and point N in Figure 1, can be formulated as $(\sqrt{A},2\sqrt{A})$ and $(1-\sqrt{B},2\sqrt{B}/K)$, respectively.

In order to obtain monotonicity of function $C(\rho)$, the relationship between $\partial C/\partial\rho$ and 0 should be considered,

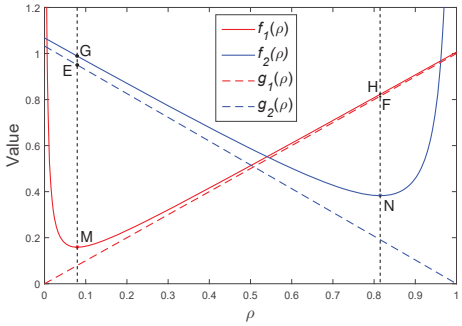

Figure 1. The graphs of $f_1(\rho)$ and $f_2(\rho)$, as well as their asymptotes $g_1(\rho)$ and $g_2(\rho)$.

which is equivalent to finding the relationship between $f_1(\rho)$ and $f_2(\rho)$. Thus, the number of intersections of $f_1(\rho)$ and $f_2(\rho)$ and the values of the intersections should be discussed, That is, the relationships between the following four algebraic expressions and 0 need to be investigated:

$$\begin{cases} f_1(0)-f_2(0), & \text{(12a)} \\ f_1(\sqrt{A})-f_2(\sqrt{A}), & \text{(12b)} \\ f_1(1-\sqrt{B})-f_2(1-\sqrt{B}), & \text{(12c)} \\ f_1(1)-f_2(1),. & \text{(12d)} \end{cases}$$

It is easy to derive that algebraic expressions (12a) and (12d) are >0 and <0, respectively, because that the values of $f_1(0)$ and $f_2(1)$ both tend to be positive infinity.

For (12b), due to the complex structure, $f_2(\sqrt{A})$ is replaced by $g_2(\sqrt{A})$, i.e, point G is replaced by point E. By simplification, it can be derived $f_1(\sqrt{A})-g_2(\sqrt{A})<0$ when

$$\begin{aligned} &\frac{8\sigma_n^2(N-2)+\pi N-\sqrt{\pi^2N^2+16\sigma_n^2\pi N(N-2)}}{4\sigma_n^2} \\ &<N_A<\frac{8\sigma_n^2(N-2)+\pi N+\sqrt{\pi^2N^2+16\sigma_n^2\pi N(N-2)}}{4\sigma_n^2}. \end{aligned} \tag{13}$$

It can be derived $f_1(\sqrt{A})-g_2(\sqrt{A})<0$ is true for all the possible N_A in its range of values when $\sigma_n^2<\pi N(4(N-3)^2)$, resulting $f_1(\sqrt{A})-f_2(\sqrt{A})<0$ because $g_2(\rho)<f_2(\rho)$ is established for any $0\le\rho\le1$.

For (12c), due to the complex structure, $f_1(1-\sqrt{B})$ is replaced by $g_1(1-\sqrt{B})$, i.e, point H is replaced by point F. By insertion, it can be derived $g_1(1-\sqrt{B})-f_2(1-\sqrt{B})>0$ when

$$\begin{aligned} &\frac{-\left(2D^2\sigma_n^2(N-2)+N\right)-\sqrt{8D^2\sigma_n^2N(N-2)+N^2}}{2D^2\sigma_n^2} \\ &<N_A<\frac{-\left(2D^2\sigma_n^2(N-2)+N\right)+\sqrt{8D^2\sigma_n^2N(N-2)+N^2}}{2D^2\sigma_n^2}. \end{aligned} \tag{14}$$

It can be derived $g_1(1-\sqrt{B})-f_2(1-\sqrt{B})>0$ is true for all the possible N_A in its range of values when $\sigma_n^2<(2N^2-8N)/(D^2(3N-4)^2)$, resulting in $f_1(1\sqrt{B})-f_2(1-\sqrt{B})>0$ because $f_1(\rho)>g_1(\rho)$ is true for any $0\le\rho\le1$.

In summary, it can be derived that

$$\begin{cases} f_1(0)-f_2(0)>0, & \text{(15a)} \\ f_1(\sqrt{A})-f_2(\sqrt{A})<0, & \text{(15b)} \\ f_1(1-\sqrt{B})-f_2(1-\sqrt{B})>0, & \text{(15c)} \\ f_1(1)-f_2(1)<0. & \text{(15d)} \end{cases}$$

when

$$\sigma_n^2<\min\left(\frac{\pi N}{4(N-3)^2},\frac{2N^2-8N}{D^2(3N-4)^2}\right), \tag{16}$$

which is easy to be satisfied under the assumption of high SNR. Thus there must be three intersections for the two graphs based on (15b,15c) and the double hook characteristic, as shown in Figure 1.

Assume that the three intersections of $f_1(\rho)$ and $f_2(\rho)$ are at $\rho=\rho_1$, ρ_2, and ρ_3 (in ascending order), respectively, which means $f_1(\rho)=f_2(\rho)$ at the three points. Therefore, ρ_1, ρ_2, and ρ_3 are also the 3 roots for

$$\frac{\partial C}{\partial\rho}=0, \tag{17}$$

and can be calculated through the formula of extracting roots because that $\partial C/\partial\rho=0$ is a simple cubic equation. Since $\partial C/\partial\rho\propto[1/f_1(\rho)-1/f_2(\rho)]$ according to (7) and Figure 1, it is obvious that

$$\frac{\partial C}{\partial\rho}\begin{cases} <0, & \rho\in(0,\rho_1)\cup(\rho_2,\rho_3) \\ >0, & \rho\in(\rho_1,\rho_2)\cup(\rho_3,1) \end{cases}. \tag{18}$$

Hence, the capacity function $C(\rho)$ decreases monotonously when $\rho\in(0,\rho_1)\cup(\rho_2,\rho_3)$, while it increases monotonously when $\rho\in(\rho_1,\rho_2)\cup(\rho_3,1)$. Thus, the maximum capacity $C_m=\max(C(0),C(\rho_2),C(1))$, while the optimal optical power allocation factor ρ_0 to maximize the total channel capacity can be achieved only at $\rho_0=0$, ρ_2, or 1.

4 Simulation Results

Simulation results were performed to evaluate the performance of the proposed scheme. W, N, N_0, and β are set as 100 MHz, 128, 10^{-10}) A^2/Hz, and 9 dB, respectively. Under this circumstance, it can be calculated that σ_n^2 is around 2.8×10^{-9}, while the right part of (16) is approximatively 0.0064, which means inequality (16) is established in this case.

The capacity performance versus ρ as well as the optimal optical power allocation factors calculated through (17) are

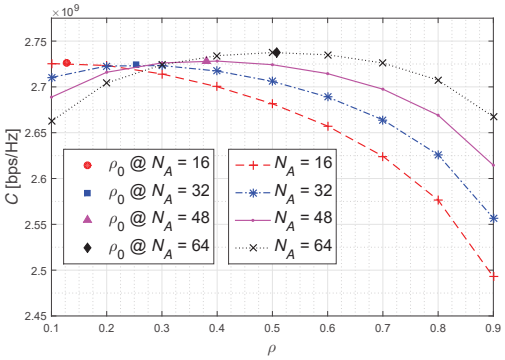

Figure 2. The relationship between ρ and the total capacity C for different N_A.

shown in Figure 2. The optimal ρ_0 for $N_A = 16$, 32, 48, and 64 are 0.127, 0.254, 0.381, and 0.508, respectively. As shown in the figure, ρ_0 obtained by (17) is exactly the optimal power allocation factor with maximum channel capacity. Because ρ_1 and ρ_3 are extremely close to 0 and 1, respectively, the monotonicity between $(0, \rho_1)$ and $(\rho_3, 1)$ are not obvious. For the conventional ADO-OFDM with $N_A = 64$, the optimal ρ_0 is 0.508, which is very close to equal power allocation, thus there is little difference in capacity performance between schemes with or without power allocation. However, for other $N_A \neq 64$, the total channel capacity with optimal optical power allocation can be significantly increased compared with that with equal power allocation.

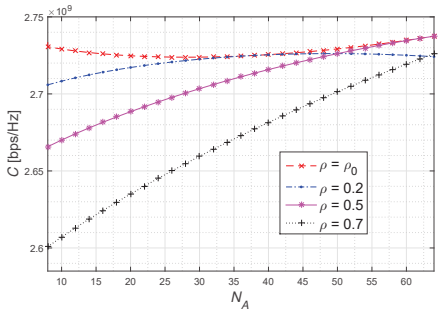

Figure 3. The relationship between N_A and the total capacity C for different ρ.

The capacity performance versus N_A at different ρ is shown in Figure 3. As shown in the figure, for the systems with the proposed power allocation factor, the total capacity decreases and increases when N_A varies from 8 to 28 and 28 to 64, respectively. For any N_A, compared with other power allocation schemes, the proposed scheme with $\rho = \rho_0$ has the optimal performance to maximize the total capacity. Specially, the total channel capacity of the system with proposed power allocation factor is significantly higher than that of the system without power allocation, i.e., $\rho = 0.5$.

5 Conclusions

In this paper, a resource allocation scheme, called enhance ADO-OFDM, for the heterogeneous network based on the compatibility of VLC and RF communication systems in the physical layer, is proposed. Additionally, the optimization of optical power allocation for the enhanced ADO-OFDM with a limit on the total optical power is analyzed. Simulation results show that the total channel capacity of the proposed scheme has a large increase compared with that of the schemes without power allocation.

6 Acknowledgements

This work is based upon research supported by the National Key Research and Development Program of China (Grand No.2017YFE0113300).

References

[1] L. Hanzo, H. Haas, S. Imre, D. O'Brien, M. Rupp, and L. Gyongyosi, "Wireless Myths, Realities, and Futures: From 3G/4G to Optical and Quantum Wireless," *Proc. IEEE*, **100**, Special Centennial Issue, May 2012, pp. 1853–1888, doi:10.1109/JPROC.2012.2189788.

[2] S. D. Dissanayake and J. Armstrong, 'Comparison of ACO-OFDM, DCO-OFDM and ADO-OFDM in IM/DD systems," *J. Lightwave Technol.*, **31**, 7, April 2013, pp. 1063–1072, doi:10.1109/JLT.2013.2241731.

[3] R. Jiang and Z. Wang and Q. Wang and L. Dai, "A tight upper bound on channel capacity for visible light communications," *IEEE Commun. Lett.*, **20**, 1, Jan 2016, pp. 97–100, doi:10.1109/LCOMM.2015.2497694.

[4] X. Li and J. Vucic and V. Jungnickel and J. Armstrong, "On the capacity of intensity-modulated direct-detection systems and the information rate of ACO-OFDM for indoor optical wireless applications," *IEEE Trans. Commun.*, **60**, 3, March 2012, pp. 799–809, doi:10.1109/TCOMM.2012.020612.090300.

[5] J. Armstrong, "OFDM for optical communications," *J. Lightwave Technol.*, **27**, 3, Feb 2009, pp. 189–204, doi:10.1109/JLT.2008.2010061.

[6] A. Weiss and A. Yeredor and M. Shtaif, "Iterative symbol recovery for power-efficient DC-biased optical OFDM systems," *J. Lightwave Technol.*, **34**, 9, May 2016, pp. 2331–2338, doi:10.1109/JLT.2016.2521768.

[7] L. Chen and B. Krongold and J. Evans, "Performance analysis for optical OFDM transmission in short-range IM/DD systems," *J. Lightwave Technol.*, **30**, 7, April 2012, pp. 974–983, doi:10.1109/JLT.2012.2185779.